International Journal of Dental Sciences
www.dentaljournal.in
E-ISSN: 2663-4708, P-ISSN: 2663-4694
Received: 22-09-2025, Accepted: 22-10-2025, Published: 06-11-2025
Volume 7, Issue 4, 2025, Page No. 112-119

Determination of density that generates artifacts in tomography in the presence of different intraradicular materials

Tatiana Siavichay Gómez[1], María Soledad Peñaherrera Manosalvas[2]
[1] Department of Endodontics, University Hemisferios, Quito, Ecuador
[2] Department of Endodontics, Director of the postgraduate program in Endodontics at the University of Los Hemisferios, Quito, Ecuador

Abstract
The main objective of the study was to evaluate the presence of artifacts in cone beam computed tomography (CBCT) images and their relationship with the density of the materials used in endodontic treatments. Three types of materials were analyzed: gutta-percha, fiberglass posts, and metal posts, in order to identify which generates more artifacts and which can interfere with anatomical structures and affect diagnosis.
Thirty-six donated human premolars that had been extracted for orthodontic treatment were used. They were disinfected with sodium hypochlorite solution and water and prepared biomechanically. Gutta-percha and NeoSealer Flo® bioceramic cement were used for the filling. The teeth were divided into three groups: G1, filled only with gutta-percha and cement; G2, with fiberglass posts; and G3, with metal posts. CBCT images were obtained by placing the teeth in a resin-printed jaw perforated to simulate alveoli, covered with pink wax and immersed in water to simulate soft tissue. A 4x4 cm field of view (FOV) was used.
The results showed that the most frequent artifact was glare, followed by noise and metal artifact. Although glare was more common, metal objects generated the highest percentage of artifacts. The standard technique presented 9.6% artifacts, while the high-definition (HD) technique showed 6.8%. Noise was predominant in the standard technique (60.5%) and almost nonexistent in the HD technique (3.7%).
With regard to materials, the percentages were similar: gutta-percha (36.1%), metal (31.0%), and fiberglass (29.2%). No statistically significant differences were found between the techniques, materials, or their interactions ($p > 0.05$), suggesting that all materials evaluated have comparable behavior in generating artifacts in CBCT.

Keywords: Cone-Beam Computed Tomography, Gutta-Percha, artifacts, *in vitro*, materials testing, root canal obturation

Introduction

The history of computed tomography (CT) dates back to 1967, when engineer Sir Godfrey Newbold Hounsfield developed a device that processed multiple X-ray beams to obtain two-dimensional images of soft tissues in living organisms, using sensors instead of X-ray film (Bosch, 2004) [1]. By capturing multiple images from a rotating photon source, slices were generated that showed the different densities of the tissues (Alarcón & Durán, 2021) [2]. These images enabled the creation of three-dimensional representations. In this way, Hounsfield established the first CT equipment for clinical practice, enabling the examination of the skull and constituting an important advance for the medical community (Nicholls, 2019) [3]. This first equipment required approximately nine days to generate the tomography and more than two hours to process the data. Years later, in 1979, the CT scanner received the Nobel Prize in Physiology or Medicine (Martinez Mondragon *et al*., 2023) [4].

Cone beam computed tomography (CBCT) has become an essential diagnostic tool, notable for offering a lower radiation dose compared to conventional CT and producing effective three-dimensional images of oral bone structures (Bali *et al*., 2023) [5]. Consequently, its application in endodontics is particularly relevant, as it provides slices in different planes (axial, coronal, and sagittal), allowing for a more accurate diagnosis of various pathologies. In addition, it is essential in planning endodontic surgeries and in recognizing root anatomy, thus increasing the chances of successful treatment (Kail *et al*., 2017) [6].

Despite the high quality and fidelity of the images produced by tomography, obvious distortions may occur in the analysis of the slices, known as artifacts (Vázquez *et al*., 2023) [7]. Artifacts are images that appear in the tomographic analysis but are not present in the actual object; they are discrepancies that arise between the physical conditions of the CBCT and the composition and behavior of the object being analyzed. The way in which the beam of rays passes through materials depends largely on their density, such as restorations, metal posts, prostheses, and implants, which can be interpreted as false positives (Crespo *et al*., 2015) [8].

Therefore, the analysis of artifacts is of utmost importance, as image distortion decreases image quality and can result in misdiagnosis (Schulze *et al*., 2011) [9]. Furthermore, the identification and understanding of these artifacts can prevent repeated patient exposure (Bali *et al*., 2023) [5]. An artifact is characterized by its sunbeam-like appearance, forming a halo from a sequence of bands (Likubo *et al*., 2020) [10]. Another type of distortion that occurs in tomography is noise, which manifests
as randomly arranged lines and stripes. As noise increases, high-density objects (such as bone) are visualized with low contrast, while soft tissues become difficult to identify (Sartori *et al*., 2015) [11]. Artifacts in CBCT images are classified into three categories: those derived from physics during data acquisition, those related to patient characteristics in terms of anatomy and position, and those associated with scanner performance (Kuteken *et al*., 2015) [12].

In view of the above, this study aims to determine the presence of artifacts in CBCT images and their relationship with the density of different materials such as gutta- percha, fiberglass posts, and metal posts used in root canals, and to find out which produces the greatest number of artifacts that can interfere with different anatomical structures and alter the diagnosis.

Materials and Methods

An *in vitro* comparative experimental study was conducted with a total of 36 lower premolars obtained from extractions performed for orthodontic treatment, through donation. te single-root, straight teeth were selected; a tooth preservation protocol for studies was applied, which recommends handling the teeth in a solution of chlorine and water in a ratio of 1:10. The teeth were then cleaned of tissue debris using an ultrasonic unit

Fig 1: Teeth cleaning and disinfection process

Fig 2: Cleaning of tissue residues with ultrasound

The teeth were then autoclaved for 40 minutes at 121°C in sterilization bags. The respective universal biosafety precautions such as gloves, mask, and eye protection were used when handling extracted teeth before use.

Fig 3: Sealed, labeled, and sterile bags.

The experimental process began with the determination of the working length and biomechanical preparation of the canals of each of the premolars. A combination of manual and reciprocating techniques was used to shape each root canal.

Fig 4: Sequence of opening (a) and manual (b) and mechanical (c) instrumentation

For root canal filling, gutta-percha cones and NeoSealer Flo® bioceramic cement were used, applying the lateral condensation technique.

The sample will be randomly divided into three groups:

G1: (N=12) premolars that were filled with gutta-percha cones and NeoSealer Flo® cement using the lateral condensation technique. They were completely sealed with SZ Cavity Base Lining LC ionomer and Solare resin and will be stored in 4 x 6 cm Ziploc bags for later evaluation.

G2: (N=12) premolars filled with gutta-percha cones and NeoSealer Flo® cement, which underwent partial removal of the cervical and middle thirds, and a size 0.5 Whitepost (FGM) fiberglass post was cemented using Relyx® resin-modified glass ionomer cement. They will then be stored in 4 x 6 cm Ziploc bags for evaluation.

G3: (N=12) premolars filled with gutta-percha cones and NeoSealer Flo® cement that underwent partial removal of the cervical and middle thirds to remove the intracanal material, in order to prepare space for a metal post. The ideal apical length that should remain inside the canal will be 4 to 5 mm, after which the metal post will
be cemented using Relyx® resin-modified glass ionomer cement. These will also be stored in 4 x 6 cm Ziploc bags for later evaluation.

Perforations simulating alveoli arranged along the jaw were made in a resin-printed jaw; the conventional surgical system with a conical connection (Morse cone) from Titaniumfix (bfox profile) was used, employing the sequence of burs from the spear bur, then with the A 2.0, B 2.0/2.5, C 2.2/2.8, D 2.8/3.4, B1 cortical 3.0, C1 cortical 3.5 burs, up to the D1 cortical 4.0 bur. The teeth from each group, correctly identified, were placed inside these perforations, located according to their material in an alternating manner (gutta-percha, fiberglass, and metal post). This location will facilitate the obtaining of CBCT images of 4 teeth per tomography due to the FOV (4x4) selected from the Newtom Giano HR Professional tomography equipment.

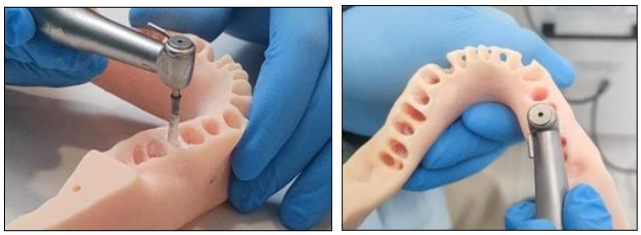

Process of drilling alveoli in a resin jaw using the conventional Titaniumfix (bfox profile) surgical system

Prior to image acquisition, the jaw was covered with pink wax and placed in a rectangular plastic box that was completely filled with water in order to simulate soft tissue, as tissues with a high-water content, such as muscles, blood, and some organs, have a density similar to that of water (0 Hounsfield Units). As a reference in radiology, the unit of measurement for density is the Hounsfield Unit (HU), which quantifies the attenuation of X-rays in body tissues, facilitating their identification in tomography images.

Fig 6: Top view (a), front view (b), and side view (c) of jaw covered with pink wax and placed in water to simulate soft tissue

Fig 7: Image of jaw covered with pink wax and placed in a rectangular plastic box with water, covered with plastic

The images were obtained in standard definition (SD) and high definition (HD) and analyzed using the NNT viewer software of the Newtom HR Professional tomographic equipment. Images were generated in coronal, axial, and sagittal sections and in the cervical, middle, and apical thirds. Artifacts were classified as noise, metal object artifacts, and glare.

The data obtained were compiled in several Excel tables designed specifically for the study, and confidence interval techniques between proportions (for presence) and contrast using confidence intervals for averages (for density) were used for data processing. The free software R v4.5.1 available at the time was used.

The hypothesis is that tomographic analysis of premolars with similar anatomy and different intracanal materials will allow for the evaluation of artifacts or distortions in the images obtained by CBCT, contributing to diagnosis and image navigation.

Fig 8: Gutta-percha in HD axial, sagittal, and coronal sections

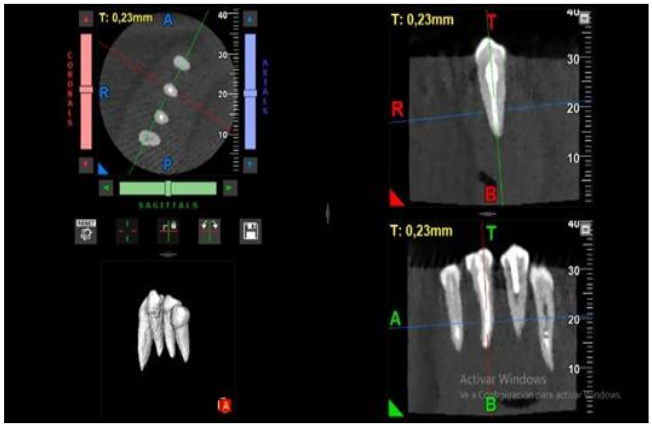

Fig 9: Gutta-percha in standard axial, sagittal, and coronal sections

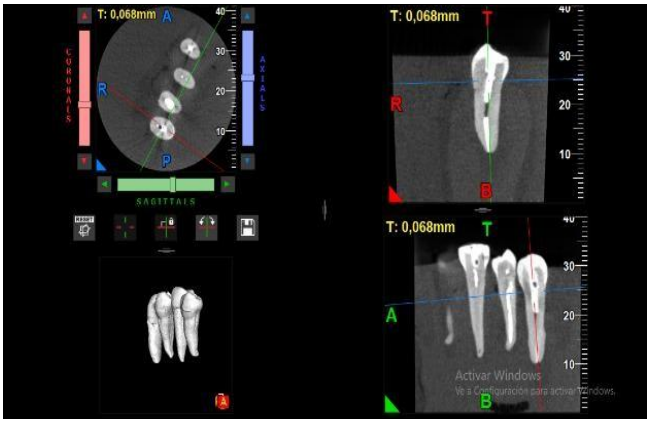

Fig 10: Metal in HD

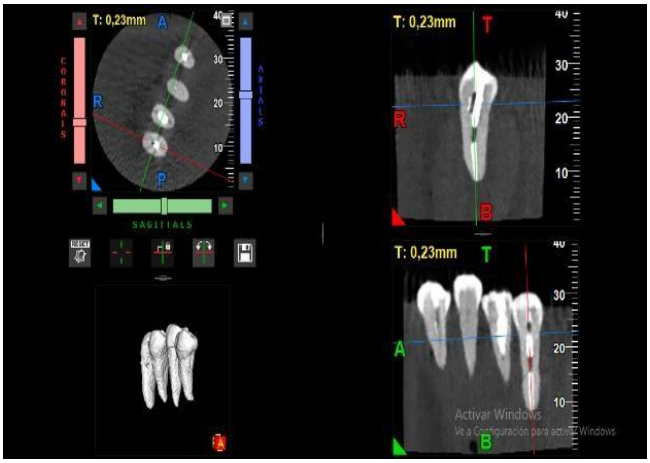

Fig 11: Metal in standard

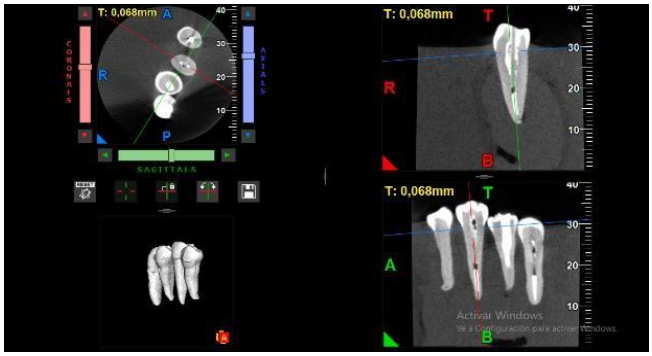

Fig 12: Fiber in HD

Fig 13: Fiber in standard

Results

According to the artifacts generated through the images obtained in CBCT, glare was the artifact that occurred most frequently in HD quality, with 8% compared to 4.6% in SD quality. According to the type of material, glare occurred in the gutta-percha group at a high rate of 10.6% compared to 6% for fiberglass and 2.3% for metal. On the other hand, the artifact produced by metallic objects occurred at a higher percentage in SD (9.6%) than in HD (6.8%).

Noise was more prevalent in navigation, with 60.5% in SD compared to 3.7% in HD. In terms of the different materials, the figures were similar between gutta-percha (36.1%), metal (31.0%), and fiber (29.2%).

The three root thirds showed high and comparable percentages (25.5–37.0%), as did the different sections (27.8–37.0%).

Finally, when analyzing the presence of artifacts per tooth, it was observed that glare tended to occur more frequently than noise and metallic artifacts. However, statistical comparisons between techniques, materials, and their interactions did not show statistically significant differences ($p > 0.05$). (See Table 2.)

Table 1: Percentage of artifacts present according to factor variables

Artifact	Factor	Variable	Measuremts	Presentation	Percentage
Flash	Techniqu e	Standard	324	15	4.6
		HD	324	26	8.0
	Material	Fiber	216	13	6.0
		Gutta-percha	216	23	10.6
		Metal	216	5	2.3
	Third	Apical	216	1	0.5
		Cervical	216	32	14.8
		Medium	216	8	3.7
	Cut	Axial	216	36	16.7
		Crown	216	5	2.3
		Sagittal	216	0	0.0
		Standard	324	31	9.6
Metallic	Technical	HD	324	22	6.8
	Material	Fiber	216	0	0.0
		Gutta-percha	216	0	0.0

		Metal	216	53	24.5
	Third	Apical	216	0	0.0
		Cervical	216	46	21.3
		Medium	216	7	3.2
	Cut	Axial	216	28	13.0
		Crown	216	17	7.9
		Sagittal	216	8	3.7
Noise	Technique	Standard	324	196	60.5
		HD	324	12	3.7
	Material	Fiber	216	63	29.2
		Gutta-percha	216	78	36.1
		Metal	216	67	31.0
	Third	Apical	216	55	25.5
		Cervical	216	73	33.8
		Medium	216	80	37.0
	Cut	Axial	216	76	35.2
		Crown	216	72	33.3
		Sagittal	216	60	27.8

95% confidence interval

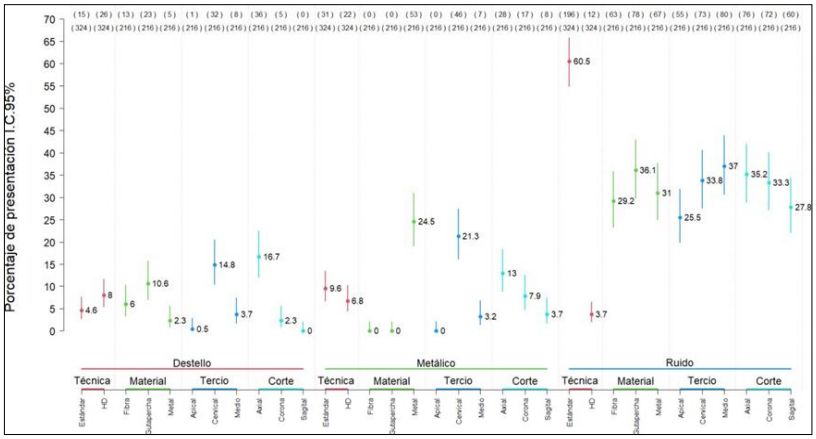

Graph:1 Percentage of presence according to factor variables.

It is interesting to evaluate the presence in each dental piece analyzed; therefore, regardless of the third or cut, the presence of each artifact is obtained according to the technique and/or material. The percentage of presence for the interaction of factors is also highlighted

Table 1: Percentage of presence according to variables of factors and interactions

Artifact	Factor	Variable	Measurements	Presentation	Percentage	p.value
Flash	Technique	Standard	36	13	36.1	0.809
		HD	36	15	41.7	
	Material	Fiber	24	11	45.8	0.081
		Gutta-percha	24	12	50.0	
		Metal	24	5	20.8	
	Technical Material	Standard-Fiber	12	5	41.7	0.209
		Standard- Gutta-percha	12	6	50.0	
		Standard-Metal	12	2	16.7	
		HD-Fiber	12	6	50.0	0.357
		HD-Gutta- percha	12	6	50.0	
		HD-Metal	12	3	25.0	
Metallic	Techni que	Standard	36	1	2.8	0.112
		HD	36	6	16.7	
	Material	Fiber	24	0	0.0	0.000
		Gutta-percha	24	0	0.0	
		Metal	24	7	29.2	
	Techni cal Material	Standard-Fiber	12	0	0.0	0.358
		Standard- Gutta-Percha	12	0	0.0	
		Standard-Metal	12	1	8.3	
		HD-Fiber	12	0	0.0	0.108
		HD-Gutta-percha	12	0	0.0	
		HD-Metal	12	6	50.0	
Noise	Techni cal	Standard	36	2	5.6	0.154
		HD	36	7	19.4	
	Materi al	Fiber	24	5	20.8	0.218
		Gutta-percha	24	3	12.5	
		Metal	24	1	4.2	

	Techni que Material	Standard-Fiber	12	1	8.3	0.589
		Standard- Gutta-Percha	12	1	8.3	
		Standard-Metal	12	0	0.0	
		HD-Fiber	12	4	33.3	0.289
		HD-Gutta-percha	12	2	16.7	
		HD-Metal	12	1	8.3	

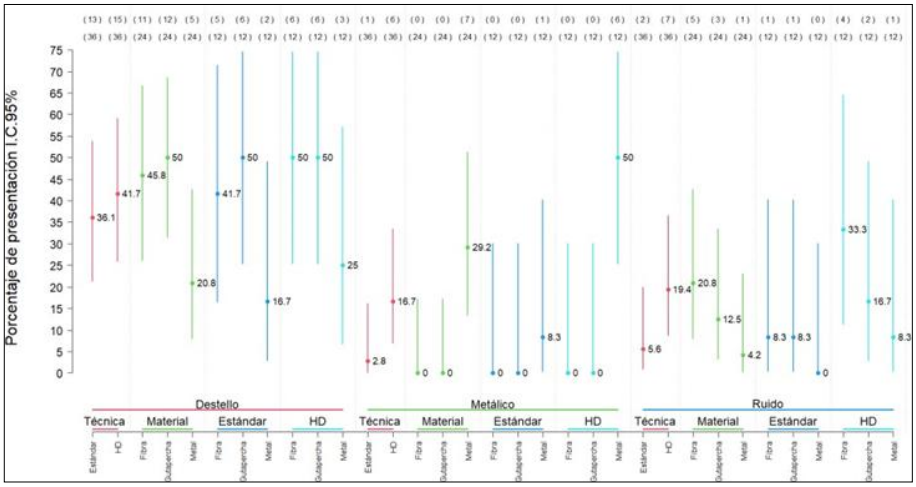

Graph 2: Percentage of presence according to factor variables and interactions

On the other hand, for the evaluation of density, values that do not include artifacts are analyzed. These refer to reference values that quantify the attenuation of X-rays represented in Hounsfield Units (HU) according to the material and technique. It should be noted that the HD technique shows a lower reference value than the Standard technique.

Table 2: Reference values for density

Technique	Average
Standard	1854
HD	1605

The following table shows the basic descriptive statistics of the assessments made according to technique and material. It shows that teeth whose interior material is fiber tend to give lower (average) values than metal and gutta-percha.
It should be noted that the coefficients of variation (CV) are relatively low, indicating that the results are relatively homogeneous in terms of technique and material levels. To visualize the distribution of the assessments made, the boxplot (box and whisker) of the values is shown, noting that in both techniques, the fiber values tend to be lower than gutta-percha and metal. It can also be seen that gutta-percha ratings tend to be the most variable in both techniques. In addition, averages and 95% CI of the reference values are shown, highlighting that fiber values are around of the reference
values and that gutta-percha and metal data are well above the reference values.
(Graph 3.)

Table 4: Descriptive statistics of densities by technique and material

Technique	Material	Samples	Average	S.D.	C.V.	p.value
Standard	Fiber	12	1532.7	290.7	19.0	0.004
	Gutta-percha	12	8034.1	2565.1	31.9	0.000
	Metal	12	14,601.7	741.5	5.1	0.000
HD	Fiber	12	1657.2	300.8	18.2	0.620
	Gutta-percha	12	9468.7	3305.7	34.9	0.000
	Metal	12	14,452.0	1234.4	8.5	0.000

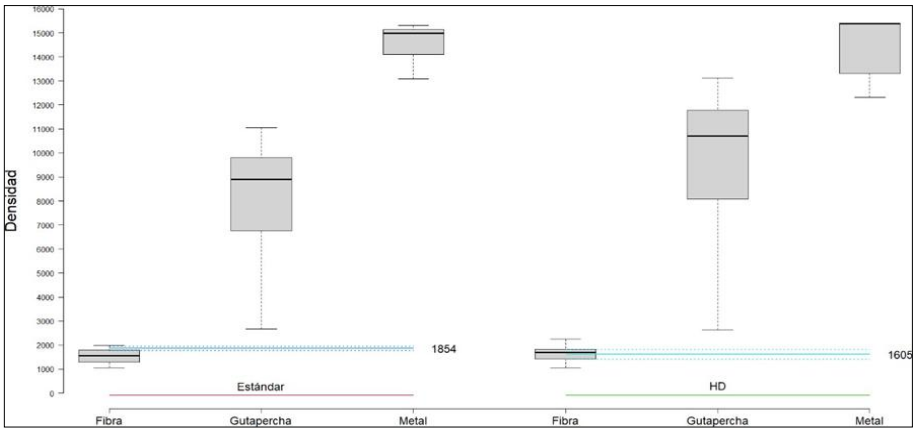

Graph 3: Density distribution according to material by technique

Discussion

This *in vitro* study evaluated the presence of artifacts produced by three materials: gutta-percha, fiberglass posts, and prefabricated metal posts in images obtained using CBCT. Based on the results, noise was shown to be the most frequent artifact, with a marked difference between the standard technique (60.5%) and the HD technique (3.7%). Flare artifact occurred mainly in gutta-percha (10.6%), followed by fiberglass (6.0%) and, to a lesser extent, metal posts (2.3%). The metal artifact was observed only in teeth with metal posts (24.5%), especially in the cervical third. In terms of density, fiberglass showed values close to the reference values, while gutta- percha and metal recorded significantly high densities.

These findings are consistent with those reported in the literature, as described by Sutare *et al*. (2023) [14] in their study, where gutta-percha produces mild artifacts, mainly around the material without significant image distortion. Similarly, Gaêta-Araujo *et al*. (2020) [15] noted that without the application of metal artifact reduction (MAR) algorithms, gutta-percha does not generate artifacts of sufficient intensity for reduction to be effective, which coincides with the variability and limited magnitude observed in our study.

In contrast, metal posts were the material that generated the highest number and density of artifacts, which is consistent with several studies. Gaêta-Araujo *et al*. (2020) [15] reported that metal artifacts are more intense in proximity to the tooth due to the beam hardening effect. Fontenele *et al*. (2021) [16] and Helvacioglu-Yigit *et al*. (2022) [17] also confirmed that metal alloys, especially those with a higher atomic number such as gold and silver-palladium, produce more artifacts compared to fiber posts and gutta-percha. These results support the findings of our research, where metal posts had much higher densities than other materials and artifacts exclusive to this group.

With regard to gutta-percha, studies such as those by Kuo *et al*. (2024) [18] and AlMohareb *et al*. (2022) [13, 19] indicated that this material generates artifacts, but to a lesser degree, and with low image distortion, although they may appear hypodense (dark bands) or hyperdense (white lines), especially in the cervical third.

Our results confirm the presence of these artifacts, predominantly in the cervical third and with densities intermediate between fiber and metal. On the other hand, fiberglass posts showed the lowest artifact production, a finding in line with that reported by Helvacioglu-Yigit *et al*. (2022) [17], who observed that fiberglass posts generate fewer artifacts than metal ones, and with what was described by AlMohareb *et al*. (2022) [13, 19], who noted less density variability in this group.

In this study, fiber presented values close to the reference values and statistically lower than gutta-percha and metal in the standard technique, reinforcing its advantage in radiology. Another aspect to consider is the influence of acquisition parameters. While previous studies highlight that factors such as tube current, FOV, and the presence of artifact reduction algorithms influence the expression of artifacts. (Gaeta-Araujo *et al*. 2020; AlMohareb *et al*. 2022) [13, 19], in our study, no statistically significant differences were observed between acquisition techniques (HD vs. standard). This discrepancy could be attributed to the *in vitro* study design and the standardization of experimental conditions.

Conclusions

In conclusion, artifacts in CBCT vary depending on the intraradicular material, with noise being the most frequent in the standard technique (60.5%) and practically absent in the HD technique (3.7%). Flicker, depending on the material, occurred more frequently in gutta-percha (10.6%), while the metallic artifact was exclusive to metal posts (24.5%).

The most critical material in terms of artifact generation is metal posts, as they produce alterations in both frequency and density, particularly in the cervical third, which can compromise the diagnostic interpretation of adjacent structures.

In terms of density, which is clearly related to the material, fiberglass showed values close to the reference values, whereas gutta-percha and metal posts showed significantly higher densities, confirming that materials with a higher atomic number generate greater radiographic distortion.

No statistical significance was shown between standard and HD acquisition techniques, suggesting that the determining variable in the generation of artifacts is the type of intraradicular material rather than the acquisition protocol used in CBCT.

Finally, this *in vitro* study provides useful evidence for clinical practice, although its findings should be interpreted with caution due to the absence of biological conditions such as soft tissues, patient movements, and different anatomical variations. It is recommended to complement these results with *in vivo* clinical studies that validate them in everyday diagnostic scenarios

References

1. Bosch E. Sir Godfrey Newbold Hounsfield and computed tomography, his contribution to modern medicine. Revista Chilena de Radiología,2004:10(4):183–5. Available at: www.nobelprize.org
2. Alarcón H, Durán Á. Godfrey Newbold Hounsfield. Revista Iberoamericana de Bioeconomía y Cambio Climático, 2021. Available at: https://revistaibio.com/ojs33/index.php/main/article/view/36/35
3. Nicholls M. Sir Godfrey Newbold Hounsfield and Allan M. Cormack. European Heart Journal,2019:40(26):2101–3. Available at: http://www.ncbi.nlm.nih.gov/pubmed/31280317
4. Martinez Mondragon M, Baruch Castro Guzmán Y el, Romero Ángeles B, Urriolagoitia Sosa G, Urriolagoitia Calderón G, Adolfo López Mateos P, *et al*. Methodology for the development of a biomodel using computed tomography for the anatomical structure of a lower first molar. Congreso de Ciencia y Tecnología Cuautitlán, 2023. Available at: https://virtual.cuautitlan.unam.mx/CongresoCiTec/Memorias_Congreso/Anio7_No7/Extensos/DE-02.pdf
5. Bali H, Luitel A, Upadhyaya C. Artifacts among Cone Beam Computed Tomography Images of Patients of Tertiary Care Centre: A Descriptive Cross-sectional Study. Journal of the Nepal Medical Association,2023:61(257):18–22.
6. Kail K, Rojas A, Fernando A, Guaneme B, Amilcar J, Vera V, *et al*. Design of a manual for interpreting cone beam tomography images with the Galileos system. Santo Tomás University, 2017.

7. Vázquez D, Subirán B, Pujol M, Estévez A, Nart L, Hecht P, *et al*. Correction of artifacts produced in tomographic images in dental equipment. Journal of the Mexican Dental Association,2023:80(4):204–8.
8. Crespo V, Orellana D, Rebolledo C, Araneda L. Comparison between artifacts produced in cone beam computed tomography with different intracanal materials. *In vitro* study. Yearbook of the Chilean Society of Oral and Maxillofacial Radiology,2015:18(1):8–14. Available at: https://es.scribd.com/document/633707063/Anuario-Sociedad-de-Radiologia-Oral-y-Maxilo-Facial-de-Chile-2015-Vol-18.
9. Schulze R, Heil U, Groß D, Bruellmann DD, Dranischnikow E, Schwanecke U, *et al*. Artefacts in CBCT: A review. Dentomaxillofacial Radiology,2011:40:265–73.
10. Likubo M, Kagawa T, Fujisawa J, Kumasaka A, Nishioka T, Kojima I, *et al*. Effect of exposure parameters and gutta-percha cone size on fracture-like artifacts in endodontically treated teeth on cone-beam computed tomography images. Oral Radiology,2020:36(4):344–8.
11. Sartori P, Rozowykniat M, Siviero L, Barba G, Peña A, Mayol N, *et al*. Common artifacts in computed tomography and magnetic resonance imaging. Revista Argentina de Radiología,2015:79:192–204.
12. Kuteken F, Penha N, Simões AC, Goisman S. Metallic artifact in cone beam computed tomography. Revista Odontológica de la Universidad Ciudad de São Paulo,2015:27(3):220–8.
13. AlMohareb RA, Barakat RM, Mehanny M. Quantitative analysis of cone-beam computed tomography artifacts induced by nonmetallic root canal filling materials using different fields of view: *In vitro* study. Scanning, 2022.
14. Sutare A, Parihar A, Reddy P, Singh R, Ac V. Influence of windowing and evaluation of metal artifact reduction algorithm on five different restorative materials by using different cone beam computed tomography scanners: A CBCT study. Cureus,2023:15(7):41742. Available at: http://dx.doi.org/10.7759/cureus.41742
15. Gaêta-Araujo H, Nascimento EHL, Fontenele RC, Mancini AXM, Freitas DQ, Oliveira-Santos C, *et al*. Magnitude of beam-hardening artifacts produced by gutta-percha and metal posts on cone-beam computed tomography with varying tube current. Imaging Science in Dentistry,2020:50(1):1–7. Available at: http://dx.doi.org/10.5624/isd.2020.50.1.1
16. Fontenele RC, Farias Gomes A, Rosado LPL, Neves FS, Freitas DQ. Mapping the expression of beam hardening artifacts produced by metal posts positioned in different regions of the dental arch. Clinical Oral Investigations,2021:25(2):571–9. Available at: http://dx.doi.org/10.1007/s00784-020-03494-z
17. Helvacioglu-Yigit D, Seki U, Kursun-Cakmak S, Demirturk Kocasarac H, Singh M. Comparative evaluation of artifacts originated by four different post materials using different CBCT settings. Tomography,2022:8(6):2919–28. Available at: http://dx.doi.org/10.3390/tomography8060245
18. Kuo H-Y, Lin K-L, Hsu C-Y, Fu P-S, Hung C-C, Song SJ. Volumetric analysis of artifacts from fiducial markers under cone beams computed tomography. Journal of Dental Sciences,2024:19(2):1004–11. Available at: http://dx.doi.org/10.1016/j.jds.2023.07.001
19. AlMohareb RA, Barakat RM, Mehanny M. Quantitative analysis of cone-beam computed tomography artifacts induced by nonmetallic root canal filling materials using different fields of view: *In vitro* study. Scanning,2022:2022:4829475. Available at: http://dx.doi.org/10.1155/2022/4829475.